

Study of Y-type hexaferrite $\text{Ba}_{0.5}\text{Sr}_{1.5}\text{ZnNiFe}_{12}\text{O}_{22}$ powders

Cite as: AIP Conference Proceedings **2075**, 160032 (2019); <https://doi.org/10.1063/1.5091359>

Published Online: 26 February 2019

B. Georgieva, T. Koutzarova, S. Kolev, K. Krezhov, D. Kovacheva, Ch. Ghelev, B. Vertruyen, L. M. Tran, and A. Zaleski



View Online



Export Citation

AIP | Conference Proceedings

Get **30% off** all
print proceedings!

Enter Promotion Code **PDF30** at checkout



Study of Y-type Hexaferrite $\text{Ba}_{0.5}\text{Sr}_{1.5}\text{ZnNiFe}_{12}\text{O}_{22}$ Powders

B. Georgieva^{1, a)}, T. Koutzarova^{1, b)}, S. Kolev^{1, c)}, K. Krezhov^{1, d)}, D. Kovacheva^{2, e)},
Ch. Ghelev^{1, f)}, B. Vertruyen^{3, g)}, L.M. Tran^{4, h)} and A. Zaleski^{4, i)}

¹*Institute of Electronics, Bulgarian Academy of Sciences, 72 Tsarigradsko Chaussee, BG-1784 Sofia, Bulgaria*

²*Institute of General and Inorganic Chemistry, Bulgarian Academy of Sciences, Acad. Georgi Bonchev Str., bld. 11, BG-1113 Sofia, Bulgaria*

³*Greenmat, Chemistry Department, University of Liege, 11 allée du 6 août, 4000 Liège, Belgium*

⁴*Institute of Low Temperature and Structure Research, Polish Academy of Sciences, Ul. Okólna 2, 50-422 Wrocław, Poland*

^{a)}Corresponding author: b.georgiewa@abv.bg

^{b)}tatyana_koutzarova@yahoo.com

^{c)}svet_kolev@yahoo.com

^{d)}kiril.krezhov@gmail.com

^{e)}dkovacheva@gmail.com

^{f)}chavdarghelev@yahoo.com

^{g)}b.vertruyen@ulg.ac.be

^{h)}L.M.Tran@intibs.pl

ⁱ⁾a.zaleski@int.pan.wroc.pl

Abstract. We report results from a study on the influence of the substitution of Zn^{2+} cations in the Y-type $\text{Ba}_{0.5}\text{Sr}_{1.5}\text{Zn}_2\text{Fe}_{12}\text{O}_{22}$ hexaferrite, known for strong magnetoelectric coupling, with magnetic cations, such as Ni^{2+} , on its structural and magnetic properties. Polycrystalline samples of $\text{Ba}_{0.5}\text{Sr}_{1.5}\text{ZnNiFe}_{12}\text{O}_{22}$ were synthesized by citric acid sol-gel auto-combustion. The saturation magnetization value of 54.7 emu/g at 4.2 K was reduced to 37.2 emu/g at 300 K. The temperature dependence of the magnetization at magnetic fields of 50 Oe, 100 Oe and 500 Oe were used to determine the magnetic phase transition temperature. We demonstrate that the helical spin state, believed to cause the magnetoelectric effect, can be achieved by varying the magnetic field strength within a given temperature range.

INTRODUCTION

Multiferroic materials are an exceptional class of magnetic materials where long-range magnetic and ferroelectric orders coexist, provoking the researchers' interest from both basic and practical points of view [1, 2]. The magnetoelectric multiferroics are materials that combine coupled electric and magnetic dipoles [3]. The hexaferrite $\text{Ba}_{0.5}\text{Sr}_{1.5}\text{Zn}_2\text{Fe}_{12}\text{O}_{22}$ is a member of the Y-type hexaferrites class ($\text{A}_2\text{Me}_2\text{Fe}_{12}\text{O}_{22}$), where A = Ba, Sr and Me is a divalent cation. It is an insulating ferrimagnet with a helical spin arrangement stabilized below Neel temperature of $T_N \approx 326$ K, undergoes several temperature-driven magnetic phase transitions, and is known to exhibit magnetoelectric effects close to room temperature under a low magnetic field of 0.8 T [4, 5]. Generally, the hexaferrites $\text{Ba}_2\text{Me}_2\text{Fe}_{12}\text{O}_{22}$ adopt a structural type described by the space group $R\bar{3}m$. All the cations (Me^{+2} and Fe^{+3}) are distributed over six distinct crystallographic sites: two tetrahedral sites ($6c_{IV}$ and $6c^*_{IV}$) and four octahedral sites ($3a_{VI}$, $3b_{VI}$, $6c_{VI}$, and $18h_{VI}$). The type of these divalent cations, as well as the site they occupy within the unit cell, can result in significant modifications of this material's structural and magnetic properties. The unit cell contains three formula units and is built from sequential stacking of the S and the T-blocks in a sequence of (TST'ST'S'), where the primes indicate a rotation about the *c*-axis by 120 degrees; the easy magnetization axis lies in a plane normal to the *c* axis direction [6].

The magnetic structure can be represented by two magnetic sublattice L and S blocks stacked alternately along [001], which bear, respectively, opposite large and small magnetization M .

With a view of potential applications of $\text{Ba}_{0.5}\text{Sr}_{1.5}\text{ZnNiFe}_{12}\text{O}_{22}$ multiferroic properties, we consider here the influence of the substitution of diamagnetic Zn with the magnetic cation Ni^{2+} on the structural and magnetic properties of $\text{Ba}_{0.5}\text{Sr}_{1.5}\text{ZnNiFe}_{12}\text{O}_{22}$ polycrystalline material prepared by wet chemistry. Single crystals of $\text{Ba}_{0.5}\text{Sr}_{1.5}\text{Ni}_2\text{Fe}_{12}\text{O}_{22}$ were reported to order magnetically at much higher temperatures ($T_N = 650$ K) than $\text{Ba}_2\text{Mg}_2\text{Fe}_{12}\text{O}_{22}$ ($T_N = 550$ K) [6, 7] and $\text{Ba}_{0.5}\text{Sr}_{1.5}\text{Zn}_2\text{Fe}_{12}\text{O}_{22}$ ($T_N = 326$ K) [4, 5]. Besides, at temperatures close to 300 K, the ferrimagnetic state in the $\text{Ba}_{0.5}\text{Sr}_{1.5}\text{Ni}_2\text{Fe}_{12}\text{O}_{22}$ hexaferrite rearranges into a proper screw magnetic ordered state; upon applying a magnetic field perpendicular to the hexagonal axis the magnetically induced ferroelectricity was observable reliably at low temperatures up to 175 K [7].

EXPERIMENTAL

The $\text{Ba}_{0.5}\text{Sr}_{1.5}\text{ZnNiFe}_{12}\text{O}_{22}$ polycrystalline material was synthesized by citric acid sol-gel auto-combustion. The corresponding metal nitrates were used as starting materials, and a citric acid solution was slowly added to the mixed nitrates as a chelator to form stable complexes with the metal cations. The solution was slowly evaporated to form a gel, which was dehydrated at 120 °C turning into a fluffy mass and was burned in a self-propagating combustion manner. The auto-combusted powders were annealed at 1170 °C in air.

The XRD patterns were taken at ambient temperature on a Bruker D8 diffractometer (40 kV, 30 mA) controlled by DIFFRACTPLUS software, in Bragg-Brentano reflection geometry with $\text{Cu-K}\alpha$ radiation ($\lambda = 1.5418$ Å). The morphology of the obtained material was examined by a Philips XL-30 FEG ESEM field emission environmental scanning electron microscope. The magnetic properties were measured by means of a Quantum Design PPMS magnetometer. The hysteresis measurements were conducted at 4.2 K and at room temperature. The zero-field-cooled (ZFC) and field-cooled (FC) magnetization vs. temperature (4.2 – 300 K) measurements were performed at magnetic fields of 50 Oe, 100 Oe and 500 Oe. In the ZFC protocol, the sample under study was cooled from room temperature down to 4.2 K without any magnetic field; the magnetization was measured with the temperature being raised from 4.2 K to 300 K at a heating rate of 3 K/min in the applied magnetic field. The FC curve was recorded on the same sample upon cooling from 300 K to 4.2 K in the same magnetic field.

RESULTS AND DISCUSSION

The XRD pattern (Fig. 1a) of the synthesized powder $\text{Ba}_{0.5}\text{Sr}_{1.5}\text{ZnNiFe}_{12}\text{O}_{22}$ material at room temperature was indexed successfully in the centrosymmetric $R\bar{3}m$ space group and showed the characteristic peaks corresponding to the Y-type hexaferrite structure as a main phase. The few extra peaks marked as a minor phase were identified as belonging to the spinel ZnFe_2O_4 amounting to 3.2 wt%, whose structural and magnetic properties either in bulk (normal spinel) or a nanostructured form (partially inverted spinel) are well documented [8, 9]. Zinc ferrite undergoes a transition from a paramagnetic to a non-collinear anti-ferromagnetic state at a temperature of about 10 K [9, 10] so that its presence could not noticeably affect the results, which are discussed below.

The lattice constants a and c of $\text{Ba}_{0.5}\text{Sr}_{1.5}\text{ZnNiFe}_{12}\text{O}_{22}$ are 5.567(2) Å and 42.337(3) Å, respectively. Thus, the lattice parameters decreased substantially in comparison with those of $\text{Ba}_{0.5}\text{Sr}_{1.5}\text{Zn}_2\text{Fe}_{12}\text{O}_{22}$ ($a \approx 5.86$ Å and $c \approx 43.4$ Å) [11]. As expected, due to the substitution the unit cell volume is strongly reduced because the ionic radius of Ni^{2+} (0.69 Å) is smaller than that of Zn^{2+} (0.75 Å).

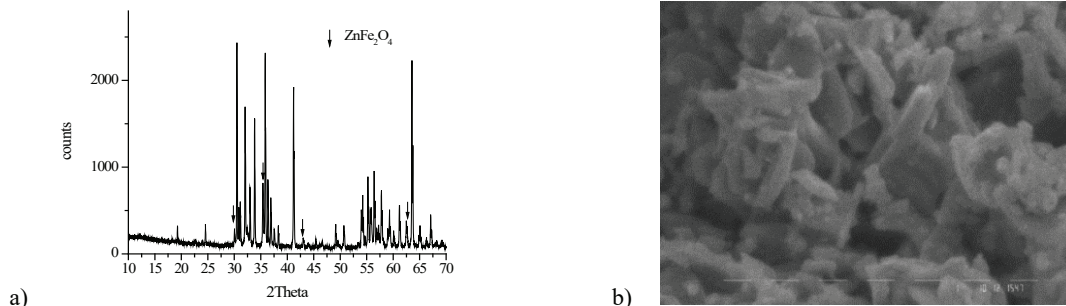


FIGURE 1. XRD pattern (a) and SEM micrograph (b) of $\text{Ba}_{0.5}\text{Sr}_{1.5}\text{ZnNiFe}_{12}\text{O}_{22}$ powder.

The SEM images showed (Fig. 1b) that the powder material obtained consists almost entirely of large hexaferrite-phase particles with a size of a few microns and clusters of submicron particles of different size and shape.

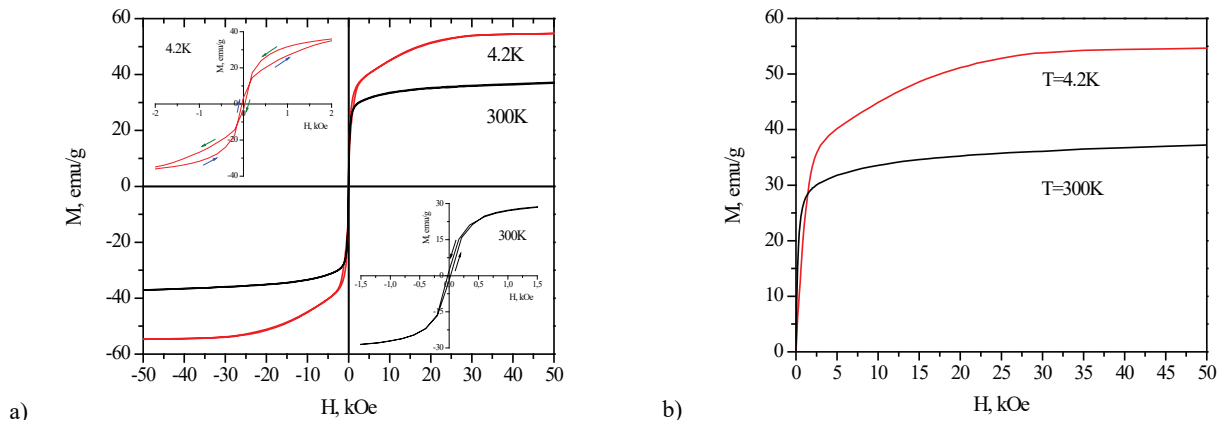


FIGURE 2. a) Hysteresis curves at 4.2 K and 300 K. The insets show the magnetization zoomed near the low magnetic field region, and b) magnetic field dependence of initial magnetization.

Figure 2 presents the initial magnetization and the hysteresis loops of the powder material at 300 K and 4.2 K. At high magnetic fields, the magnetization almost reaches saturation. The values of M_s in a magnetic field H of 50 kOe were 54.7 emu/g and 37.2 emu/g at 4.2 K and 300 K, respectively. At 300 K, the magnetization rises steeply with a rather quick stepwise growth up to $H \approx 700$ Oe and then follows the typical behavior of ferrimagnetic materials. At 4.2 K, the magnetization steeply increases up to $H \approx 1.7$ kOe and then exhibits a different behavior – a divergent tendency up to $H \approx 30$ kOe. A similar behavior has been reported for a $\text{Ba}_{0.5}\text{Sr}_{1.5}\text{Ni}_2\text{Fe}_{12}\text{O}_{22}$ single crystal at 20 K, as well as for other Y-type hexagonal ferrites with distinct magnetoelectric coupling, e.g. $\text{Ba}_{0.5}\text{Sr}_{1.5}\text{Co}_2\text{Fe}_{12}\text{O}_{22}$ [11]; this is evidence for magnetic field-induced transitions between different magnetic arrangements [7, 11].

The hysteresis curve is very narrow and characterized by a coercive field H_c of 33 Oe at 4.2 K, which is reduced to 24 Oe at 300 K. Such values are typical for the hexaferrites with planar magneto-crystalline anisotropy. This is why the Y-type hexaferrites generally meet the requirements to soft magnetic materials [6]. The inset in Fig. 2a displays a triple hysteresis loop at 4.2 K in the low magnetic field range, which indicates the presence of two kinds of ferromagnetic states with different magnetization values.

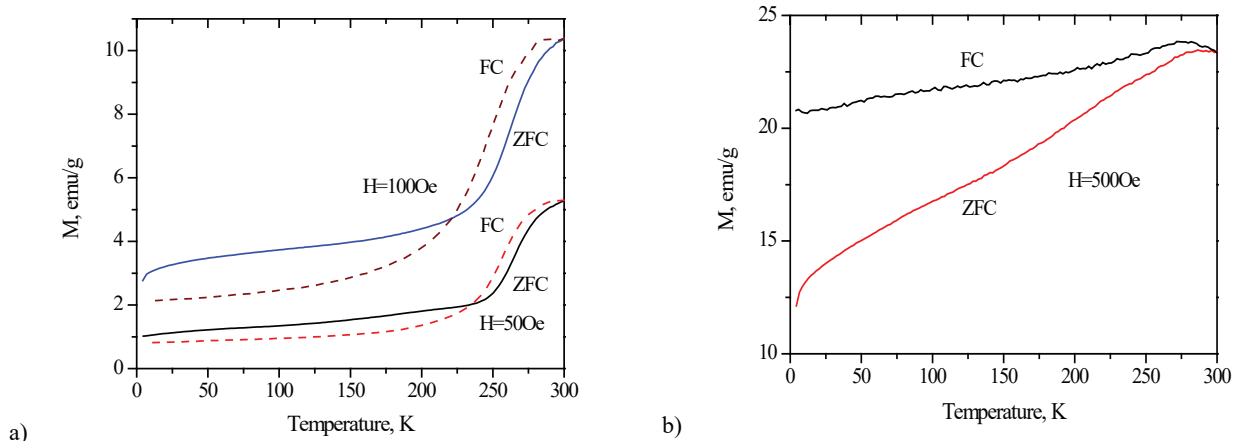


FIGURE 3. ZFC- and FC-magnetization vs temperature at a magnetic field of (a) 50 Oe and 100 Oe and (b) 500 Oe.

Figure 3 shows the temperature dependence of the ZFC and FC magnetization curves of $\text{Ba}_{0.5}\text{Sr}_{1.5}\text{ZnNiFe}_{12}\text{O}_{22}$ polycrystalline material at magnetic fields of 50 Oe, 100 Oe and 500 Oe in the temperature range 4.2 – 300 K. The magnetization curves at 50 Oe and 100 Oe (Fig. 3a) exhibit a similar behavior. The magnetization grows smoothly up

to about 200 K, when the increase becomes very steep as the temperature is raised further to 300 K. The transition temperature to a paramagnetic phase is much higher than room temperature, so this transition could not be observed. One might expect the transformation from the screw magnetic ordered state to the ferrimagnetic arrangement above room temperature to occur through successive metamagnetic transitions, with the evolution of the magnetic structures related to the magnetoelectric effect being in accordance with the findings of Hiraoka et al. [7, 11] for $\text{Ba}_{0.5}\text{Sr}_{1.5}\text{Ni}_2\text{Fe}_{12}\text{O}_{22}$.

The first derivative (not shown here) of the temperature dependence of ZFC (FC) magnetization shows a maximum at 266 K (256 K) and 263 K (250 K) for 50 Oe and 100 Oe, respectively, which determines an inflection point of the corresponding curve. In analogy with $\text{Ba}_{0.5}\text{Sr}_{1.5}\text{Zn}_2\text{Fe}_{12}\text{O}_{22}$ and $\text{Ba}_{0.5}\text{Sr}_{1.5}\text{Ni}_2\text{Fe}_{12}\text{O}_{22}$ displaying strong intrinsic magnetoelectric coupling, it might be inferred that a helical spin arrangement has set in. Accordingly, a helical spin screw magnetic order can be observed below 260 K, while between 260 K and 300 K the magnetic order adopts the so-called intermediate phase [11]. The behavior of ZFC and FC magnetization curves at a magnetic field of 500 Oe is quite dissimilar from those at low fields (Fig. 3b). It indicates that the helical spin state is quite sensitive to external manipulation and can be transformed further by increasing the magnetic field.

CONCLUSION

$\text{Ba}_{0.5}\text{Sr}_{1.5}\text{ZnNiFe}_{12}\text{O}_{22}$ polycrystalline material was obtained by citric acid sol-gel auto-combustion. The magnetization loop taken at 4.2 K showed a triple hysteresis behavior, which indicated the presence of two kinds of ferromagnetic states with different magnetization values. The temperature of transition to conical spin order known to bring about the appearance of a strong magnetoelectric coupling in undoped $\text{Ba}_{0.5}\text{Sr}_{1.5}\text{Zn}_2\text{Fe}_{12}\text{O}_{22}$ through temperature-driven metamagnetic phase transitions was determined for magnetic fields of 50 Oe and 100 Oe. The half substitution of Zn with Ni shifted this magnetic phase transition towards the higher temperatures. We established that the conical spin arrangement set in a given temperature range much above the liquid-nitrogen temperature can be further modified by a relatively low external magnetic field even below 500 Oe.

ACKNOWLEDGMENTS

B. Georgieva was supported for the synthesis, structural and microscopic properties of $\text{Ba}_{0.5}\text{Sr}_{1.5}\text{ZnNiFe}_{12}\text{O}_{22}$ by Contract DFNP-17-159 funded by the BAS under Young Scientists and Doctoral Students Assistance Program 2017. The work was supported in part by the Bulgarian National Science Fund under contract DN 08/4 “Novel functional ferrites-based magneto-electric structures”, by a joint research project between the Bulgarian Academy of Sciences and WBI, Belgium, and by a joint research project between the Bulgarian Academy of Sciences and the Institute of Low Temperature and Structure Research, Polish Academy of Sciences.

REFERENCES

1. S.-W. Cheong and M. Mostovoy, *Nat. Mater.* **6**, 13-20 (2007).
2. N. Kida, S. Kumakura, S. Ishiwata, Y. Taguchi and Y. Tokura, *Phys. Rev. B* **83**, 064422 (2011).
3. T. Kimura, *Annu. Rev. Condens. Matter Phys.* **3**, 93-100 (2012).
4. T. Kimura, G. Lawes and A.P. Ramirez, *Phys. Rev. Lett.* **94**, 137201 (2005).
5. Y. S. Chai, S. H. Chun, S. H. Haam, Y. S. Oh, I. Kim and K. H. Kim, *New J. Phys.* **11**, 073030 (2009).
6. R. C. Pullar, *Prog. Mater. Sci.* **57**, 1191-1334 (2012).
7. Y. Hiraoka, H. Nakamura, M. Soda, Y. Wakabayashi and T. Kimura, *J. Appl. Phys.* **110**, 033920 (2011).
8. S. Ligenza, M. Lukasia, Z. Kucharski, J. Suwalski, *phys. stat. sol. (b)* **117**, 465 (1983).
9. T. Kamiyama, K. Haneda, T. Sato, S. Ikeda and H. Asano, *Solid State Commun.* **81**, 563 (1992).
10. R. Raeisi Shahraki, M. Ebrahimi, S. A. Seyyed Ebrahimi and S. M. Masoudpanah, *J. Magn. Magn. Mater.* **324**, 3762–3765 (2012).
11. Y. Hiraoka, Y. Tanaka, T. Kojima, Y. Takata, M. Oura, Y. Senba, H. Ohashi, Y. Wakabayashi, S. Shin and T. Kimura, *Phys. Rev. B* **84**, 064418 (2011).
12. G. Wang, S. Cao, Y. Cao, S. Hu, X. Wang, Z. Feng, B. Kang, Y. Chai, J. Zhang and W. Ren., *J. Appl. Phys.* **118**, 094102 (2015).